



LAWRENCE  
LIVERMORE  
NATIONAL  
LABORATORY

# Deep Mixing of $^3\text{He}$ : Reconciling Big Bang and Stellar Nucleosynthesis

P. P. Eggleton, D. S. P. Dearborn, J. Lattanzio

July 31, 2006

Science

## **Disclaimer**

---

This document was prepared as an account of work sponsored by an agency of the United States Government. Neither the United States Government nor the University of California nor any of their employees, makes any warranty, express or implied, or assumes any legal liability or responsibility for the accuracy, completeness, or usefulness of any information, apparatus, product, or process disclosed, or represents that its use would not infringe privately owned rights. Reference herein to any specific commercial product, process, or service by trade name, trademark, manufacturer, or otherwise, does not necessarily constitute or imply its endorsement, recommendation, or favoring by the United States Government or the University of California. The views and opinions of authors expressed herein do not necessarily state or reflect those of the United States Government or the University of California, and shall not be used for advertising or product endorsement purposes.

# Deep Mixing of $^3\text{He}$ : Reconciling Big Bang and Stellar Nucleosynthesis

Peter P. Eggleton<sup>1,3\*</sup>, David S. P. Dearborn,<sup>2,3</sup>  
John. C. Lattanzio<sup>4</sup>

<sup>1</sup>Institute of Geophysics and Planetary Physics

<sup>2</sup>Physics and Applied Technologies Division

<sup>3</sup>Lawrence Livermore National Lab., 7000 East Ave, Livermore, CA94551, USA

<sup>4</sup>Centre for Stellar and Planetary Astrophysics, Monash University, Australia

\*To whom correspondence should be addressed; E-mail: ppe@igpp.ucllnl.org

**Low-mass stars,  $\sim 1 - 2$  solar masses, near the Main Sequence are efficient at producing  $^3\text{He}$ , which they mix into the convective envelope on the giant branch and should distribute into the Galaxy by way of envelope loss. This process is so efficient that it is difficult to reconcile the low observed cosmic abundance of  $^3\text{He}$  with the predictions of both stellar and Big Bang nucleosynthesis. In this paper we find, by modeling a red giant with a fully three-dimensional hydrodynamic code and a full nucleosynthetic network, that mixing arises in the supposedly stable and radiative zone between the hydrogen-burning shell and the base of the convective envelope. This mixing is due to Rayleigh-Taylor instability within a zone just above the hydrogen-burning shell, where a nuclear reaction lowers the mean molecular weight slightly. Thus we are able to remove the threat that  $^3\text{He}$  production in low-mass stars poses to the Big Bang nucleosynthesis of  $^3\text{He}$ .**

The standard evolution of a low-mass star (Fig. 1) takes it from a short-lived pre-Main-Sequence (PMS) state, in which it contracts and heats up but has not yet become hot enough to burn its nuclear fuel, to the long-lived MS state in which slow steady nuclear reactions keep the star in thermal equilibrium. After several gigayears (but depending strongly on mass) the nuclear fuel is exhausted at and near the center, the star becomes cooler, larger and more luminous, and it starts to climb the Red-Giant Branch (RGB). Its outer layers become turbulent and convective, and this Surface Convection Zone (SCZ) penetrates deeply into the star; but the SCZ is forced to retreat again as the fuel-exhausted core, surrounded by a thin hot nuclear-burning shell, advances outwards. During the growing phase the SCZ dredges up and homogenises material that, at the earlier MS phase, was processed by nuclear reactions in the interior.

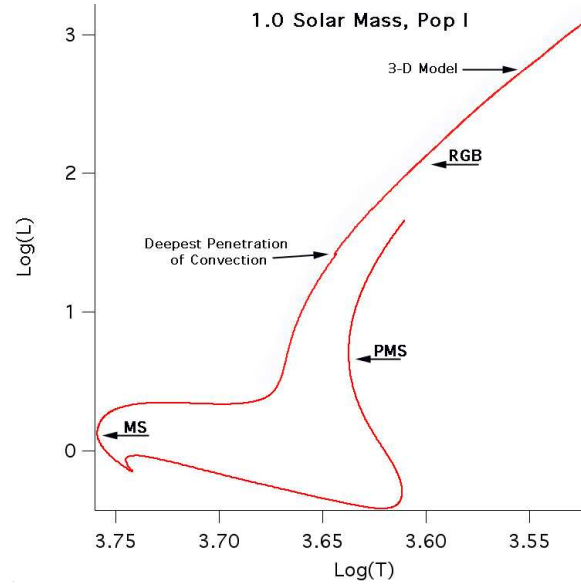


**Figure 1.** Evolution of a low-mass Pop I star in a luminosity-temperature diagram. The model was computed in 1D, i.e. spherical symmetry was assumed, using the code of (1, 2) with updated equation of state, opacity and nuclear reaction rates (3). Surface temperature is in Kelvins, luminosity in Solar units.

Along the MS stars burn hydrogen in their cores by a combination of the pp chain (in which 4 protons unite to form a  $^4\text{He}$  nucleus) and the CNO tri-cycle (in which the same process is

catalysed by carbon, nitrogen and oxygen). The former is the more important in low-mass stars,  $\lesssim 1 M_{\odot}$ , and the latter in more massive stars. However even in the more massive stars there is still a shell, somewhat outside the main energy-producing region, where the pp chain partially operates, burning H to  ${}^3\text{He}$  but not beyond.

Because the pp chain is less sensitive to temperature than the CNO cycle, cores of low-mass stars are free of convection; but convective cores develop in higher-mass stars because CNO energy production is too temperature sensitive for radiation to stably transport the energy. Above  $\sim 2 M_{\odot}$  this convective core is large enough that the  ${}^3\text{He}$  produced is convected into the center of the star and burnt there. But in stars of lower mass  ${}^3\text{He}$  accumulates (4) in a broad zone outside the main energy-producing region (Fig. 2a).  ${}^3\text{He}$  is enriched above its assumed initial value ( $2 \cdot 10^{-4}$  by mass (5), the same as its surface value in this plot) in a broad peak extending over nearly half the mass (as well as about half the radius) of the star. The maximum  ${}^3\text{He}$  abundance in this peak is a factor of  $\sim 18$  larger than the initial value.

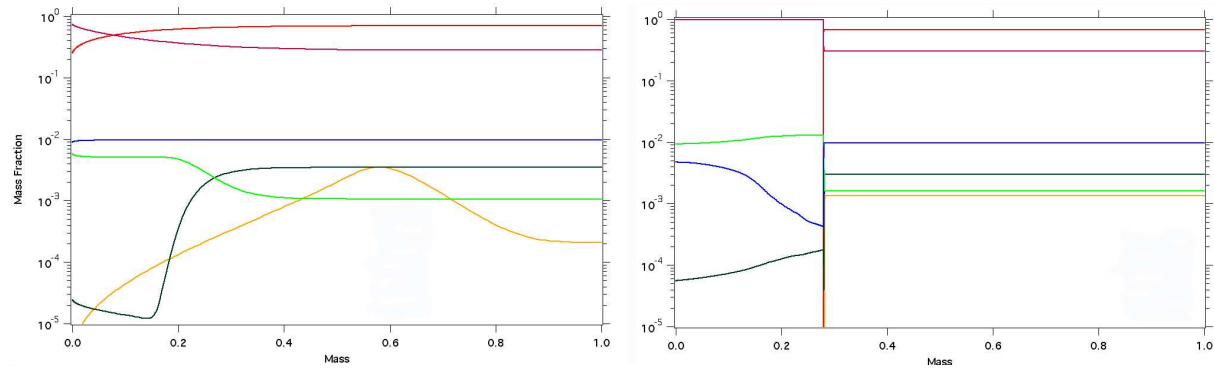


**Figure 2.** (a) Profiles of the abundances of certain nuclei in a star which has evolved to roughly the end of the MS (Fig. 1;  $T \sim 5000$  K,  $L \sim 2 L_{\odot}$ ).  ${}^1\text{H}$  is orange,  ${}^4\text{He}$  is red,  ${}^{16}\text{O}$  is blue,  ${}^{12}\text{C}$  is black,  ${}^{14}\text{N}$  is green and  ${}^3\text{He}$  is yellow.  ${}^3\text{He}$  shows a major peak where the abundance reaches  $\sim 18$  times the initial (surface) abundance. (b) The same star later, when the SCZ reaches its maximum inward extent (Fig 1).

The  $^3\text{He}$  peak has been homogenized, to a factor of 8 larger than its initial value. The inert, H-depleted core is about  $0.27 M_{\odot}$ .

On the lower part of the RGB (Fig. 1), a large SCZ develops, which mixes and homogenises the outer  $\sim 0.7 M_{\odot}$  (Fig. 2b). The surface  $^3\text{He}$  abundance is raised from the initial of  $2.10^{-4}$  to  $\sim 1.6.10^{-3}$ , i.e. by a factor of  $\sim 8$ .

As the star climbs the RGB beyond the point (Fig. 1) where the SCZ penetrates most deeply, the SCZ is diminished by (a) nuclear burning below its base, in a zone that marches outwards, and (b) stellar-wind mass loss from its surface. The evidence for the latter is that the next long-lived stage after the RGB is the Horizontal Branch (HB), and HB stars appear to have masses that are typically  $0.5 - 0.6 M_{\odot}$ , substantially less than the masses of stars capable of evolving to the RGB in less than a Hubble time (6, 7). Process (b) leads to enrichment of the interstellar medium (ISM) in  $^3\text{He}$  (8, 9, 10).

Yet the ISM's abundance of  $^3\text{He}$ , at  $\sim 5.10^{-5}$  by mass, is little different from that predicted by Big Bang nucleosynthesis. This is a major problem (11, 12): either the Big Bang value is too high, or the evolution of low-mass stars is wrong.

In this paper we identify a mechanism by which low-mass stars destroy (on the RGB) the  $^3\text{He}$  that they produced during their MS evolution. Although we illustrate this with a star like the Sun, regarding both mass and initial composition, we emphasise that exactly the same applies to low-mass metal-poor stars ('Population II'), which may have been more important than metal-rich ('Population I') stars like the Sun throughout the earlier part of Galactic history in determining the  $^3\text{He}$  abundance of the interstellar medium. The process is largely independent of mass provided it is fairly low:  $1 - 2 M_{\odot}$  for Pop I and  $0.8 - 1.6 M_{\odot}$  for Pop II.

Once the SCZ has reached its deepest extent, part-way up from the base of the RGB, it retreats, and can be expected to leave behind a region of uniform composition with  $^3\text{He}$  enhanced (Fig. 2b). This region is stable to convection according to the usual criterion that the tempera-

ture gradient should be sub-adiabatic, and is quite extensive in radius although small in mass. The H-burning front moves outwards into the stable region, but preceding the H-burning region proper is a narrow region, usually thought unimportant, in which the  $^3\text{He}$  burns. The reaction that mainly consumes it is  $^3\text{He} (^3\text{He}, 2p)^4\text{He}$ , which is an unusual reaction in stellar terms because it lowers the mean molecular weight: two nuclei become three nuclei, and the mean mass per nucleus decreases from 3 to 2. Since the molecular weight ( $\mu$ ) is the mean mass per nucleus, but including also the much larger abundances of  $^1\text{H}$  and  $^4\text{He}$  that are already there and not taking part in this reaction, this leads to a small inversion in the  $\mu$ -gradient. The inversion is tiny (Fig. 3): it is in about the fourth decimal place. But our 3D modeling shows the inversion to be hydrodynamically unstable, as we should expect from the classic Rayleigh-Taylor instability.

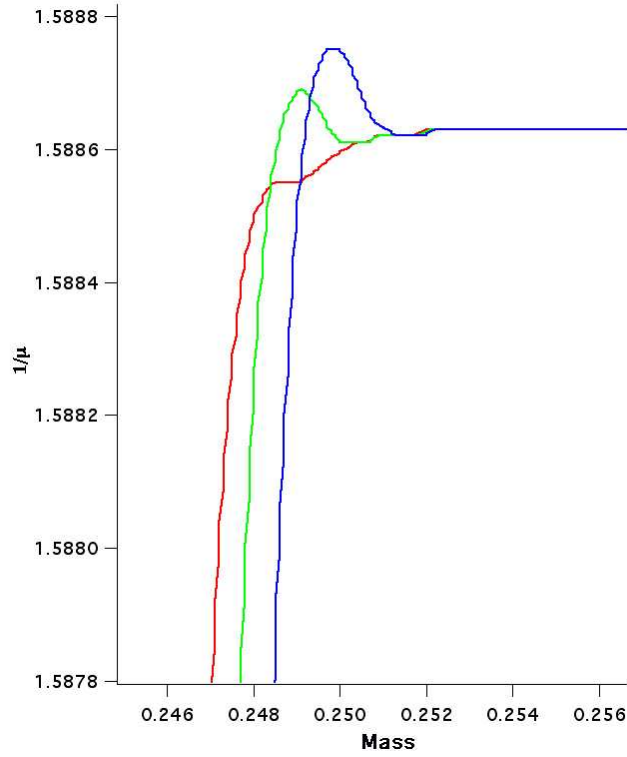


**Figure 3.** The profile of reciprocal molecular weight ( $1/\mu$ ) as a function of mass in solar units, at three successive times (red, then green 2 Myr later, then blue 2Myr later still).

At a stage (Fig. 3) when the SCZ has only just begun to retreat, there is no bump in  $1/\mu$ , but just a slight distortion at about  $0.248 M_{\odot}$ . This is because the  $^3\text{He}$  consumption is taking place in a region where there is still a substantial  $\mu$  gradient left over from earlier history. But as the H-burning shell moves out (in mass), the  $^3\text{He}$ -burning shell preceding it moves into a region of more uniform  $^1\text{H}/^4\text{He}$  ratio, and so the peak in  $1/\mu$  begins to stand out. By the time the leading edge of the shell has moved to  $0.25 M_{\odot}$  there is a clear local maximum in  $1/\mu$ , which persists indefinitely as the H-burning shell advances and the convective envelope retreats.

At a point somewhat beyond this in the evolution of our 1D star (Fig. 1) we mapped the 1D model on to a 3D model and used the hydrodynamic code ‘Djehuty’ developed at the Lawrence Livermore National Laboratory (13, 14, 15). The code is described most fully in the third of these papers. Although Djehuty is designed to deal with an entire star, from center to photosphere, we economised on meshpoints by considering only the region below the SCZ. It is important for numerical purposes that the 1D and 3D codes use exactly the same approximations for physical processes, e.g. equation of state, nuclear reaction rates, opacities.

The location of the starting model of the 3D calculation is shown on Fig. 1. If we had been clear before starting the 3D calculation that the  $1/\mu$  bump was going to cause mixing, we would have started further down, at the point where the bump first presents itself, which is just above the point labelled ‘deepest penetration’. It has become clear that our unexpected mixing will begin around here, and in practice we expect (as discussed below) that almost all of the  $^3\text{He}$  in the SCZ will have been consumed by the time the model reaches the point where our 3D calculation started. Since 3D modeling is very expensive of computer time, we have chosen not to redo the calculation for an earlier starting-point. Fig. 4 is a cross-section of the starting model for the 3D run, and shows the  $\mu$ -inversion as a ring well outside the burning shell.



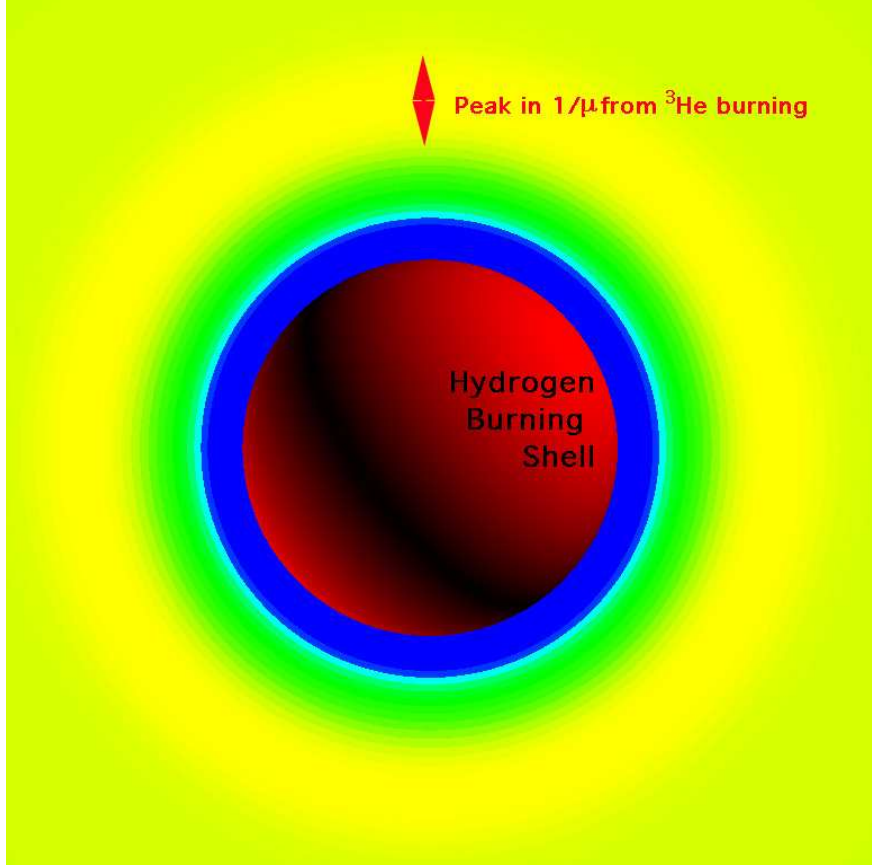


**Figure 4.** A color-coded plot of  $\mu$  on a cross-section through the initial 3D model. The shell where the  $\mu$ -inversion occurs is the yellow region sandwiched between a yellow-green and a rather darker green. The inversion is at a radius of  $\sim 5 \cdot 10^7$  m. The base of the SCZ is at  $\sim 2 \cdot 10^9$  m, well outside the frame, and the surface of the star is at  $\sim 2 \cdot 10^{10}$  m. .

Following the early development of the initially-spherical shell on which  $1/\mu$  has a constant value near its peak (Fig. 5), the surface has begun to dimple after only  $\sim 800$  secs, and by 2118 secs the dimpling is very marked and the surface has begun to tear. Some points have moved  $\sim 2\%$  radially, i.e.  $\sim 10^6$  m, indicating velocities of  $\sim 500$  m/s. The mean velocity decreases slightly in the passage from the second to the fourth panel. Other spherical shells, well away from the inversion on either side, show no such dimpling, at least until the influence of

the inversion has spread to them. A movie of which Fig. 5 is four frames is given as Movie.S1 in Supplementary Online Material.

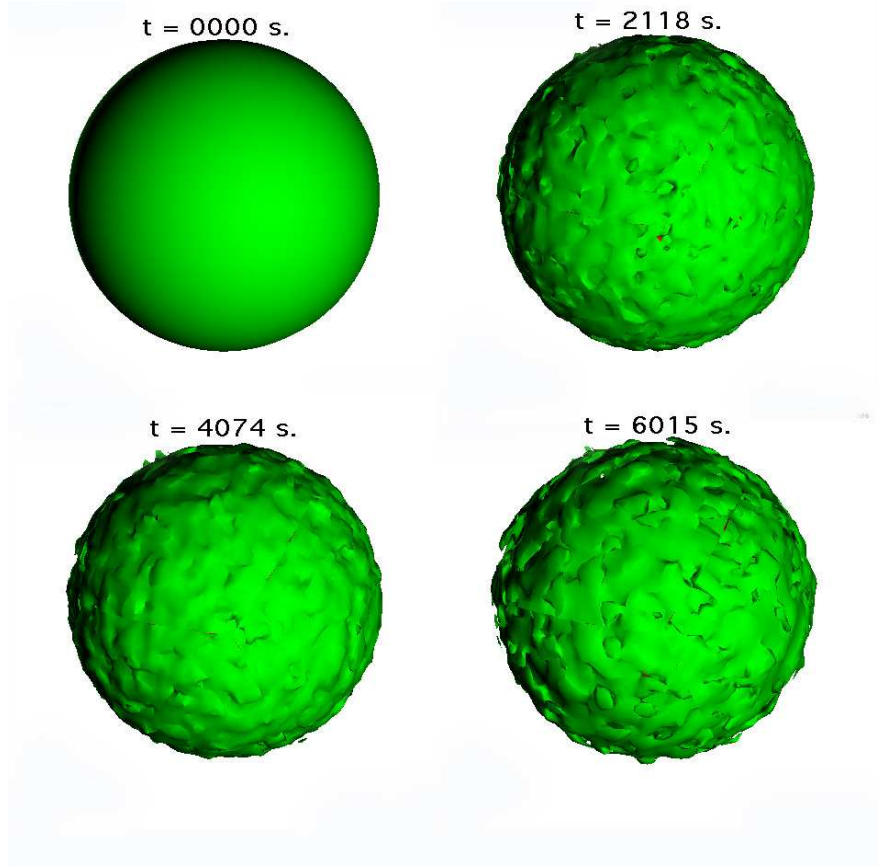


**Figure 5.** The development with time of a contour surface of mean molecular weight near the peak in the blue curve of Fig. 3. The contour dimples, and begins to break up, on a timescale of only  $\sim 2000 \text{ sec.}$

The velocity we see is roughly consistent with the expectation that it should be  $v^2 \sim gl\Delta\mu/\mu$ , where  $g$  is the local gravity and  $l$  is the local pressure scale height. The motion appears turbulent, and has the effect of diluting the inverse molecular-weight gradient, but it cannot eliminate it. As the turbulent region entrains more of the normally stable region outside it yet below the normal convective envelope, it brings in fresh  $^3\text{He}$ , which burns at the base of this mixing region, thus sustaining the inverse molecular-weight gradient. Ultimately this turbulent region will extend

to unite with the normally-convective envelope, so that the considerable reservoir of  $^3\text{He}$  there will also be depleted. If its speed of  $\sim 500$  m/s is maintained the time for processed material to reach the classically unstable SCZ is only about 1 month, while the time for the H-burning shell to burn through the  $\sim 0.02 M_{\odot}$  layer is over  $10^6$  yrs.

The above argument establishes that the mixing in the SCZ is extended below the classical convective limit, and that it is very fast compared to the nuclear timescales of either the hydrogen-burning shell or the  $^3\text{He}$ -burning reaction. We estimate from the nuclear-burning rates we find that as the hydrogen shell burns outwards the  $^3\text{He}$  will be destroyed in 16 times as much mass as the hydrogen shell burns through.

We believe that the extra mixing that we have seen gives a satisfactory answer to the problem of matching the  $^3\text{He}$  abundance of Big Bang nucleosynthesis. Although low-mass stars do indeed produce considerable amounts of  $^3\text{He}$  on the MS, this will all be destroyed by the substantially deeper mixing that we now expect on the RGB.

Our deeper mixing can also be relevant to further problems. According to the classical models of RGB stars, there is no further modification to the composition in an RGB convective envelope after it has reached its maximum extent early on the RGB. Yet observations persistently suggest that the ratios  $^{13}\text{C}/^{12}\text{C}$  and  $^{14}\text{N}/^{12}\text{C}$  both increase appreciably as one goes up the RGB (16, 17). Both these ratios can be expected to increase only if the material in the envelope is somehow being processed near the H-burning shell. Our model makes this very likely. Although the  $\mu$ -inversion that we find is somewhat above the main part of the H-burning shell, it is not far above and we can expect some modest processing of  $^{12}\text{C}$  to  $^{13}\text{C}$  and  $^{14}\text{N}$ . According to (18), it appears to be necessary for some extra mixing to take place beyond the point on the RGB where the SCZ has penetrated most deeply; that is exactly the point where our mechanism should start to operate. In (18, 19, 20, 21) it was suggested that rotation in the region between the SCZ and the hydrogen-burning shell might be responsible for the required mixing. We do

not dispute the possible importance of rotation; however we emphasise that the mechanism we have discovered is not ad hoc, but simply arises naturally when the modeling is done in 3D. This mixing occurs regardless of possible variables like rotation and magnetic fields. It seems possible to us that different rates of rotation might vary the efficiency of our process, and we intend to investigate models with rotation in the future.

Correlations between abundance excesses and deficits of various elements and isotopes in the low-mass evolved stars of globular clusters have been reported in (16). Although it is hard to distinguish star-to-star variations that may be due to evolution from those that may be due to primordial variation, we expect our mechanism to lead to substantial evolutionary variations.

We feel that our investigation demonstrates particularly clearly the virtue of attempting to model in 3D, where the motion evolved naturally, and to a magnitude that initially surprised us.

### References and Notes

1. D. S. P. Dearborn, in *The Sun in Time*, C. Sonett, M. Giampapa, M. Mathews, Eds. ISBN 0-8165-12987-3 University of Arizona Press, Tucson, AZ, USA p159 (1991)
2. P. P. Eggleton, *MNRAS* **156**, 361 (1972).
3. O. R. Pols, C. A. Tout, Zh. Han, P. P. Eggleton, *MNRAS* **274**, 964 (1995)
4. I. Iben, Jr, *Astrophys. J.* **147**, 624 (1967)
5. D. S. Balser, T. M. Bania, R. T. Rood, T. L. Wilson *Astrophys. J.* 510, 759 (1999).

The initial value for  $^3\text{He}$  that we assumed is somewhat higher than the mass-fraction ( $\sim 5 \cdot 10^{-5}$ ) implied by this reference. This is partly because we assume that primordial deuterium, of comparable abundance, is wholly burnt into  $^3\text{He}$  before the computation starts. However the important point is that the great bulk of the  $^3\text{He}$  in the RG phase is what was synthesised from ordinary hydrogen during the MS phase, and not what was

there initially. The enrichment factor of 8 that we mention above would be a factor of  $\sim 16$  if we started with half as much  $^3\text{He}$ , but the abundance level of  $\sim 1.6 \cdot 10^{-3}$  would be very much the same.

6. J. Faulkner, *Astrophys. J.* **144**, 978 (1966)
7. J. Faulkner, *Astrophys. J.* **173**, 401 (1972)
8. G. Steigman, D. S. P. Dearborn, D. Schramm, in *Nucleosynthesis and its implications on nuclear and particle physics*, J. Audouze, N. Mathieu, Eds *NATO ASI Series*. Volume C163, p37 (1986)
9. D. S. P. Dearborn, D. Schramm, G. Steigman, *Astrophys. J.* **302**, 35 (1986)
10. D. S. P. Dearborn, G. Steigman, M. Tosi, *Astrophys. J.* **465**, 887 (1996)
11. N. Hata *et al.*, *Phys. Rev. Lett.* **75**, 3977 (1995)
12. K. A. Olive, R. T. Rood, D. N. Schramm, J. Truran, E. Vangioni-Flam, *Astrophys. J.* **444**, 680 (1995)
13. G. Bazán *et al.*, in ‘3-D Stellar Evolution’ S. Turcotte, S. C. Keller, R. M. Cavallo, Eds ASP conf. **293**, p1 (2003)
14. P. P. Eggleton *et al.*, in ‘3-D Stellar Evolution’ S. Turcotte, S. C. Keller, R. M. Cavallo, Eds ASP conf. **293**, p15 (2003)
15. D. S. P. Dearborn, J. C. Lattanzio, P. P. Eggleton, *Astrophys. J.* **639**, 405 (2006)
16. N. Suntzeff, in *The globular clusters-galaxy connection*, G. H. Smith, J. P. Brodie, Eds *ASPC* **48**, 167 (1993)

17. R. P. Kraft, *PASP* **106**, 553 (1994)
18. A. Weiss, C. Charbonnel, *Mem. S. A. It.* **75**, 347 (2004)
19. A. V. Sweigart, K. G. Mengel, *Astrophys. J.* **229**, 624 (1979)
20. C. Charbonnel, *Astrophys. J.* **453**, L41 (1995)
21. P. A. Denissenkov, C. A. Tout, *MNRAS* **316**, 395 (2000)
22. We are indebted to R. Palasek for managing the code, and for assistance with the graphics. This study has been carried out under the auspices of the U.S. Department of Energy, National Nuclear Security Administration, by the University of California, Lawrence Livermore National Laboratory, under contract No. W-7405-Eng-48.

### **Supporting Online Material**

[www.sciencemag.org](http://www.sciencemag.org)

Movie S1

**Figure 1.** Evolution of a low-mass Pop I star in a luminosity-temperature diagram. The model was computed in 1D, i.e. spherical symmetry was assumed, using the code of (1, 2) with updated equation of state, opacity and nuclear reaction rates (3). Surface temperature is in Kelvins, luminosity in Solar units.

**Figure 2.** (a) Profiles of the abundances of certain nuclei in a star which has evolved to roughly the end of the MS (Fig. 1;  $T \sim 5000$  K,  $L \sim 2 L_{\odot}$ ).  $^1\text{H}$  is orange,  $^4\text{He}$  is red,  $^{16}\text{O}$  is blue,  $^{12}\text{C}$  is black,  $^{14}\text{N}$  is green and  $^3\text{He}$  is yellow.  $^3\text{He}$  shows a major peak where the abundance reaches  $\sim 18$  times the initial (surface) abundance. (b) The same star later, when the SCZ reaches its maximum inward extent (Fig 1). The  $^3\text{He}$  peak has been homogenized, to a factor of 8 larger than its initial value. The inert, H-depleted core is about  $0.27 M_{\odot}$ .

**Figure 3.** The profile of reciprocal molecular weight ( $1/\mu$ ) as a function of mass in solar units, at three successive times (red, then green 2 Myr later, then blue 2Myr later still).

**Figure 4.** A color-coded plot of  $\mu$  on a cross-section through the initial 3D model. The shell where the  $\mu$ -inversion occurs is the yellow region sandwiched between a yellow-green and a rather darker green. The inversion is at a radius of  $\sim 5 \cdot 10^7$  m. The base of the SCZ is at  $\sim 2 \cdot 10^9$  m, well outside the frame, and the surface of the star is at  $\sim 2 \cdot 10^{10}$  m. .

**Figure 5.** The development with time of a contour surface of mean molecular weight near the peak in the blue curve of Fig. 3. The contour dimples, and begins to break up, on a timescale of only  $\sim 2000$  sec.